# An Overview of Sub-100 mV Oscillators

Marcio Bender Machado[1], Rafael Luciano Radin[2]

[1]IFSP – Federal Institute of Sao Paulo, Campus Campinas, SP, Brazil
[2] UFSC – Federal University of Santa Catarina, Electrical Engineering Department, Florianopolis, Brazil,
e-mail: marciobma@gmail.com

***Abstract*—This paper presents a comprehensive review of the state of the art for oscillators operating at reduced supply voltage. The analysis and implementation examples of different types of oscillators, such as LC oscillators, transformer-based oscillators, and CMOS oscillators are presented. Expressions for the oscillation frequency and the minimum supply voltage limit are provided. The characteristics, advantages, and constrains of different topologies are discussed, providing a reference guideline for the choice of the best topology for a given application.**

***Index Terms*—Ultra low voltage; oscillator; energy harvesting; LC-oscillator; ring oscillator; minimum startup; sub-100 mV.**

## I. Introduction

Oscillators are essential building blocks in analog and digital design commonly employed to provide the clock source in several synchronous circuits or provide a carrier signal that modulates the baseband signals to the intermediate frequency (IF) or radiofrequency (RF) in communication transceivers. Motivated by IoT applications, where the power reduction is fundamental to increase circuit autonomy, examples of sub-100 mV oscillators applied to ultra-low-power (ULP) communication circuits were recently presented in [1] and [2].

Oscillators operating at the sub-100 mV range also found an important application in energy-harvesting converters due to their ability to self-start at extremely low supply voltages [3]. In such an application, the AC outputs of ULV oscillators are connected to voltage multipliers, generating a boosted DC supply voltage that can directly supply low power loads, as is shown in Fig. 1 (a). Another option is to power the control circuit of a main efficient converter in a complete energy harvesting interface, as shown in Fig. 1 (b), enabling its startup. In the application, the minimum $V_{DD}$ required to achieve oscillations is the most relevant figure of merit of the oscillator. Several design techniques were reported in the literature to reduce the minimum $V_{DD}$.

Due to a new range of applications for oscillators operating from ultra-low voltages, some recent works reported CMOS oscillators operating from DC voltages below 100 mV. Employing transistors with near-zero threshold voltages and using back bias tunning to reduce the minimum $V_{DD}$, a CMOS ring oscillator (RO) operating from around 100 mV was presented in [4]. The work described in [5] uses a

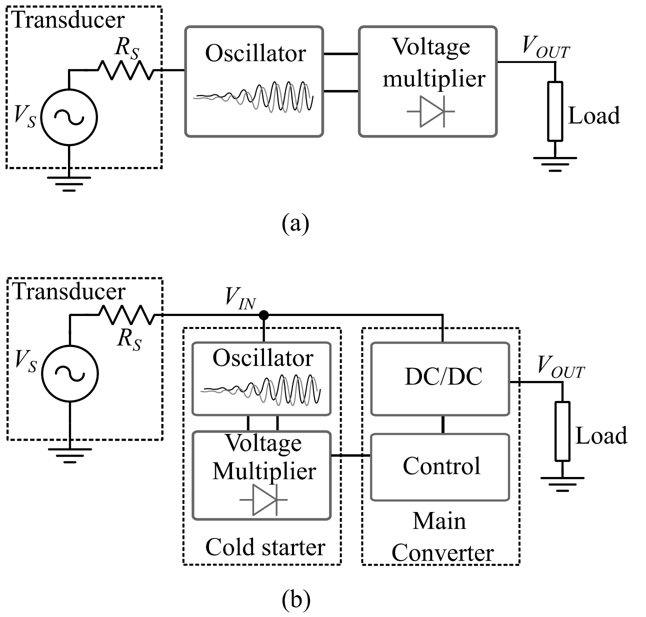


Fig. 1 Sub-100 mV oscillators applied to energy scavenging circuits. In (a), the ULV oscillator is employed in the main power path; In (b), a hybrid converter topology, employing a ULV oscillator in the cold-starter block.

VT-tuned CMOS oscillator with a hot-carrier injection that achieves startup for $V_{DD}$ at the order of 80 mV. The minimum $V_{DD}$ of CMOS oscillators was further reduced in [6] by the adoption of a stacked inverter topology and in [7] and [8] by using Schmitt trigger (ST) cells.

Although several works based on CMOS ring oscillators report operation for voltages below 100 mV, further reduction in the minimum supply voltage is possible by adopting LC-based ULV oscillators based on native transistors and off-chip capacitors, inductors, or transformers. For example, in [9], a proof-of-concept oscillator reports the achievement of oscillations from a supply voltage of 5.5 mV using JFET transistors and bulk transformers. In addition, recent works report the operation of topologies such as the Colpitts oscillator from DC voltages of the order or lower than 20 mV [10], [11], [12], and the enhanced-swing cross-coupled oscillator (ES-XCO) [3], [13] from voltages as low as 3.5 mV and 31 mV, with off-the-shelf and fully integrated inductors, respectively.

This paper presents a comprehensive review of state of the art for oscillators operating at voltages below 100 mV. The remainder of this paper is divided as follows: Section II presents LC oscillators circuit examples and then analyzes, providing expressions for the minimum $V_{DD}$ and oscillation

Digital Object Identifier 10.29292/jics.v17i1.577

frequency. Transformer-based oscillators and CMOS ring oscillators are discussed in Sections III and IV, respectively. Section V presents other oscillator topologies operating at low supply voltage. At the end, we provide a comparison between different types of oscillators in Section VI.

## II. LC Oscillators

In recent years, ultra-low-voltage (ULV) oscillators based on LC-tank topologies were presented. Some characteristics such as high peak amplitude (higher than the supply rails), high impedance load in the resonance frequency, and the possibility to start up from voltages far below 100 mV; make the LC oscillators very attractive to energy harvesting circuits [14], [15], [16], [17], [18], [19], but not limited to this application.

On the other hand, the inductor size in a fully integrated implementation, or the need for external inductors according to the minimum voltage specification, can constrain the use of this kind of circuit.

Throughout this section, low or zero-VT MOSFETs were used to obtain the necessary drive capability to sustain oscillations at voltages of the order of a few millivolts. Off-the-shelf JFET can also be found in some implementations.

In this section, we present the essential characteristics and some implementations of ULV LC arrangements, the cross-coupled oscillator (XCO), also known as inductive ring oscillator (IRO) for two or more amplifier stages, the enhanced swing cross-coupled oscillator (ES-XCO), and single-ended oscillators.

### A. Cross-coupled oscillator

The XCO, shown in Fig. 2, is one of the most used topologies for generating AC signals from DC voltages below 100 mV [1], [3], [13], [20], [21], [22], [23]. Based on two common-source tuned amplifiers, the circuit provides two out-of-phase outputs, which is desirable for connecting to voltage multipliers in energy harvesting converters.

The expressions for the oscillation frequency (ω) and the minimum supply voltage limit ($V_{DD,lim}$) of the XCO are given in (1) and (2), respectively [3]. $C$ is the sum of all parasitic capacitances between the drain node and the AC ground, $\phi_t$ is the thermal voltage, and $n$ is the transistor slop factor. We assumed operation in weak inversion [24] and negligible losses of the passive components for the derived expressions.

$$\omega = \frac{1}{\sqrt{LC}}, \quad (1)$$

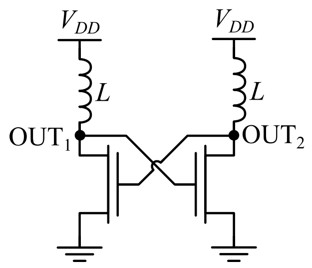


Fig. 2 Schematic diagram of the cross-coupled oscillator.

$$V_{DD,lim} = \phi_t \ln[1 + n]. \quad (2)$$

Some implementations with the circuit shown in Fig. 2 were published in the last years. The work presented in [20] reports the achievements of oscillations for a minimum voltage supply of 53 mV using a seven-stage IRO. Fig. 3 shows the micrograph of the fully integrated IRO implemented in a 130 nm process. An implementation of the XCO built with off-the-shelf inductors, operating from 50 mV, is presented in [3]. In [13], a fully integrated XCO, also implemented in the 130 nm process, achieves oscillation from 46 mV.

Some XCO connected to voltage multipliers are presented in the literature. In [22] and [23], fully-integrated oscillators, operating from 100 mV and 65 mV, respectively, are employed to startup inductive converters. In [21] and [25], oscillators connected to voltage multipliers are used to power microwatts loads directly.

Fully integrated crossed-coupled oscillators working from less than 100 mV were also explored for applications in communication circuits. In [1], XCO consuming only 20 µW of DC power was presented. The prototype oscillates at 400 MHz and is designed for wireless body area network applications using the MICS band. In [2], the design and simulation of an XCO employing low-VT transistors were presented, achieving oscillations at 2.45 GHz.

### B. Enhanced swing cross-coupled oscillator

The ES-XCO is a variation of the XCO circuit presented in the former subsection, as shown in Fig. 4. Due to the inclusion of an additional inductor per stage ($L_2$), the oscillator can boost the signal amplitude to a much higher value than the voltage supply. Also, the minimum $V_{DD}$ is reduced to the order of a few millivolts, as experimentally verified in some references [3] [13] [14] [18] [26] [27].

The ω and $V_{DD,lim}$ of the topology are given by (3) and (4), respectively [3]. As assumed for the XCO calculation, the equations consider lossless passive devices and the MOSFET operation in weak inversion. As seen in (4), $V_{DD}$ has no hard minimum limit and depends on the inductance ratio $L_2/L_1$. However, the inductor losses constrain the voltage limit of practical implementations, especially in a fully-integrated design.

$$\omega = \frac{1}{\sqrt{(L_1 + L_2)C}}, \quad (3)$$

$$V_{DD,lim} = \phi_t \ln\left(1 + n\frac{L_1}{L_1 + L_2}\right). \quad (4)$$

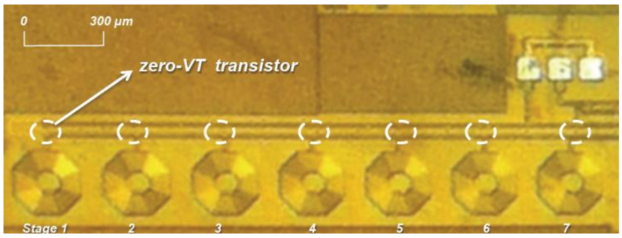


Fig. 3 The seven-stage IRO implemented in the 130 nm process.

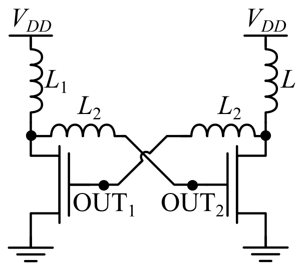


Fig. 4 Schematic diagram of the enhanced-swing cross-couped oscillator.

An ES-XCO working from 3.5 mV is presented in [3]. The prototype employs large zero-VT transistors and high-quality factor discrete inductors with a large inductance ratio ($K_L$= $L_2$/$L_1$ = 100), resulting in a considerable voltage swing at the output. A fully-integrated version of the ES-XCO oscillating from 31 mV is presented in [13]. A low inductance ratio ($K_L$≈4) was designed in the implementation. In [14], [18], [26], and [27], versions of the ES-XCO coupled to the Dickson charge pumps were presented. The fully-integrated circuit in [27] started up from voltages below 73 mV. In [18] and [26], the converter's output voltages of the order of 500 mV are obtained from input voltages smaller than 11 mV. In the former two publications, zero-VT transistors and off-the-shelf inductors were employed.

### *C. Single-ended oscillators*

Versions of classical single-ended oscillators were also designed for energy harvesting circuits.

Fig. 5 shows the schematic diagram of the ULV Colpitts and the Hartley oscillators. In both circuits, as only one active element is used, the Barkhausen criteria of zero overall phase-shift is obtained with the help of the passive network.

The oscillation frequency and the minimum voltage limit of the Colpitts oscillator shown in

Fig. 5 (a) are given in (5) and (7), respectively. Similar to the ES-XCO, there is no hard voltage limit for the Colpitts topology.

$$\omega = \frac{1}{\sqrt{LC_{eq}}}, \qquad (5)$$

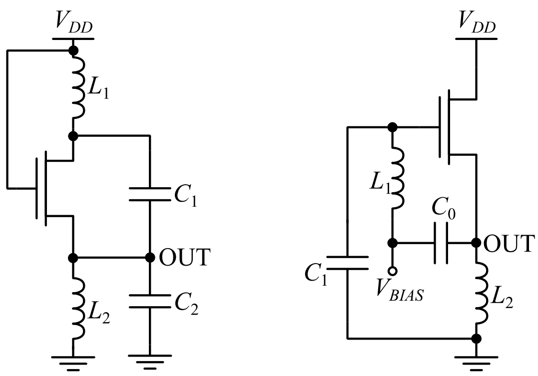


(a) (b)

Fig. 5 Schematic diagram of the (a) Colpitts oscillator (b) Hartley oscillator.

where, for the case which $L$=$L_1$=$L_2$

$$C_{eq} = C_1 + \frac{C_2}{2} - C_1\sqrt{1 + \left(\frac{C_2}{2C_1}\right)}, \qquad (6)$$

$$V_{DD,lim} = \phi_t \ln\left(1 + \frac{C_2/C_1}{1 + L_1/L_2}\right). \qquad (7)$$

Some implementations of the circuits of

Fig. 5 show the operation with some dozens of millivolts. In [10] and [11], discrete implementations of the Colpitts achieved oscillations from $V_{DD}$ lower than 20 mV. A fully integrated version of the same circuit reported oscillations from 86 mV [12]. In [28], the Colpitts oscillator was employed in a cold start converter, oscillating from DC voltages of 40 mV. The Hartley oscillator of

Fig. 5 (b), mounted with off-the-shelf devices, is employed in a DC-DC boost converter [29]. Using a commercial JFET, the converter can start up from 24 mV.

## III. Transform-Based Oscillators

Transformer-based oscillators, inspired by the classical Armstrong or Meissner oscillators, have been proposed in the literature targeting ULV energy harvesting applications. The circuits, which are versions of LC-Tank oscillators, present some advantages for ULV design. For example, the transformer AC gain in the feedback network increases the voltage swing at the gate terminal, allowing the saturation of the MOSFET at very low supply voltages. Also, the increase in the output peak amplitude decreases the number of voltage-multiplier stages in a typical energy-harvesting implementation. However, the area increment of a bulky transformer can constrain the use of the topology. Fig. 6, shows some sub-100 mV implementations of the transformer-based oscillators published in recent years [30], [31], [32], [33], [34] and [35]. Like the oscillators presented in Section III, zero-VT MOSFET or JFET were employed in most designs.

The circuit of Fig. 6 (a) has been employed in some ULV harvesters. Based on this topology, the off-the-shelf TC 3108 DC/DC converter provides a regulated output voltage from inputs of 20 mV, building an interface for thermoelectric generators or small solar cells [30]. With miniaturized high turns-ratio transformers, the same circuit was used in a cold start converter [31], [32] or the main converter [33], [34] working from less than 50 mV. In addition, a unity-ratio transformer was adopted in the circuit of Fig. 6 (b) [35]. The cross-coupled transformer-based oscillator shown in Fig. 6 (c) is presented [36].

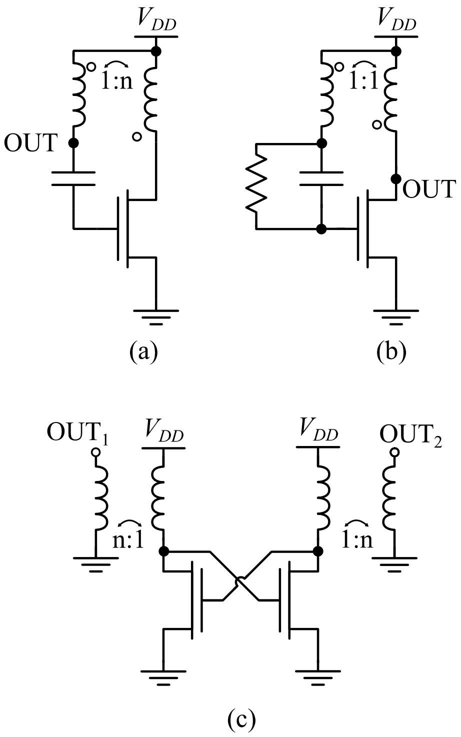


Fig. 6 Implementations of transformer-based oscillator in energy harvesting applications.

## IV. CMOS RING OSCILLATORS

Ring oscillators based only on CMOS inverters (Fig. 7) have some advantages over the LC-based oscillators. Since the circuit is implemented without any passive component, its area is significantly reduced. Also, the well-known circuit analysis and no additional technical requirements make the implementation easy and the circuit very popular. On the other hand, the minimum DC voltage presented in recent publications is around 60 mV, higher than the minimum limit obtained for LC oscillators. Low phase noise and low-frequency operation are also some usual constraints of the CMOS oscillator topologies.

For a symmetrical inverter of Fig. 7 operating in weak inversion, the voltage gain $g_m/g_o$ of each stage is given by [37]

$$\frac{g_m}{g_o} = \left(e^{V_{DD}/2\phi_t} - 1\right)/n \ . \tag{8}$$

From (8), the limit for the minimum $V_{DD}$ is obtained

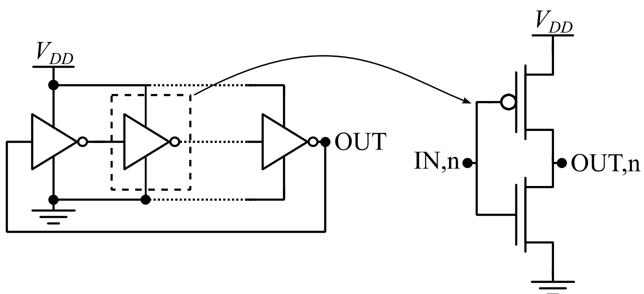


Fig. 7 Schematic diagram of a ring oscillator.

when $g_m/g_o = 1$, and it is given by [37]

$$V_{DD,lim} = 2\phi_t \ln[1 + n] \ . \tag{9}$$

Equation (9) is the Meindl limit of the CMOS inverter [38]. For $n$=1 and at room temperature, the voltage limit of the topology is 36 mV.

The DC voltage reduction of the topology has been studied extensively. From (8), the minimum inverter voltage gain is reduced with $V_{DD}$ decrease. Therefore, efforts have been made to increase each stage's voltage gain and reduce the minimum DC voltage of the topology. In [4], researchers demonstrated its operation from around 100 mV using an experimental process. In [5] and [39], the minimum supply voltages of 95 mV and 80 mV, respectively, were obtained employing a post-layout process to tune the threshold voltage of the circuit transistors. In [40], an auxiliary pull-up and down network controls the process variation. This network, controlled by a corner detector, is implemented in the circuit, helping the ring oscillator to start at 60 mV. As implemented in [37] and [41], the stage gain also increases with bulk polarization.

### A. *Enhanced voltage gain stages*

Some circuit topologies have been used to increase the voltage gain of one RO stage. Schmitt Trigger (ST) inverters have been employed to decrease the ring oscillator minimum voltage. With an optimized design, the minimum voltage for unitary voltage gain in the ST of Fig. 8, is $2\phi_t \ln\left[\left(8 + \sqrt{73}\right)/9\right]$. At room temperature, this value is equal to 31.5 mV [7], which is a little below the Meindl limit given by (9). In [42], [7], and [37], ring oscillator implementations employing ST cells have sustained operation for voltage supplies of 70 mV, 57 mV, and 53.2 mV, respectively.

A stacked-inverter RO operating from $V_{DD}$=57 mV is presented in [6]. As shown in

Fig. 9, each oscillator stage is composed of three inverters, in which the leakage current from the output node to the AC ground is reduced, increasing the stage voltage gain [43].

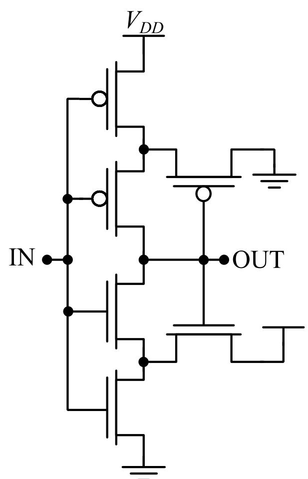


Fig. 8 Schematic diagram of the classical Schmitt Triger.

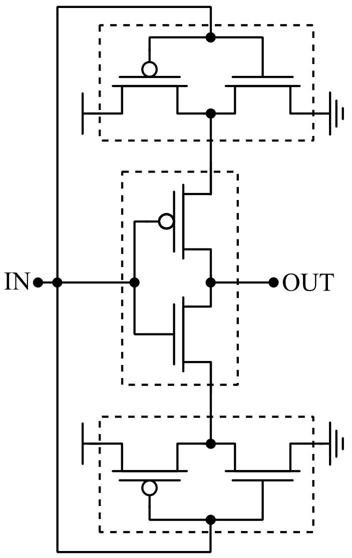


Fig. 9 Schematic diagram of one stage of the stacked-inverter ring oscillator [43].

## V. Other Oscillator Implementations

### *A. Relaxation Oscillators*

Relaxation oscillators can also operate from DC voltages below 100 mV. Using a three-inverter Schmitt Trigger shown in Fig. 10 (a), an oscillator able to start from 62 mV was reported in [44]. In the schematic shown in Fig. 10 (b), the ST is followed by a two-stage inverter that operates as a voltage-controlled current source (VCCS), along with an off-chip capacitor.

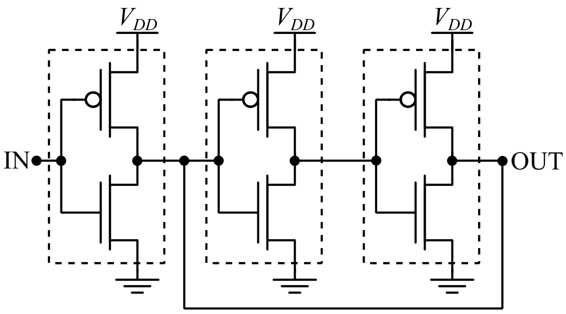


(a)

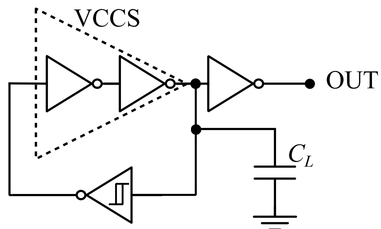


(b)

Fig. 10 Schematic diagram of the: (a) three-inverter Schmitt Trigger; (b) relaxation oscillator [44].

### *B. Cristal-based Oscillator*

Crystal-based oscillators are useful blocks employed in many clock circuits. Some works have recently presented topologies working from ULV DC levels, motivated by low-power IoT applications. The Pierce oscillator shown in Fig. 11 employs the classical Schmitt Trigger to increase the inverter voltage gain, as presented in [45]. The 32-kHz oscillator operates from a 60-mV supply voltage, consuming 2.26 nW.

Another implementation of the crystal-based oscillator using a PLL is presented in [46]. The 32-kHz circuit oscillates at 100 mV, consuming 1.7 nW of overall power. However, the PLL requires a second supply of 400 mV. In [47], an off-the-shelf implementation, employing a crystal and a transformer oscillates from a supply voltage of 17 mV.

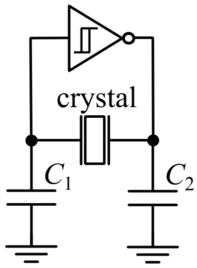


Fig. 11 Pierce crystal oscillator.

## VI. Discussion

A comparison between sub-100 mV oscillators presented in this review is shown in Tables 1 and 2 for fully integrated and external components implementations, respectively. As can be seen in both tables, the minimum supply voltage was obtained with the ES-XCO, which started at only 3.5 mV in an implementation employing native transistors from the 130 nm process and high-quality external inductors. Using external components, the ES-XCO was the only topology to operate at voltages lower than 20 mV, at the expense of 4 inductors. For fully-integrated implementations, the topology also had the minimum start-up voltage; however, CMOS oscillators based on Schmitt trigger and stacked inverters decrease the gap between LC and CMOS-based oscillator's minimum DC voltage.

Transformer-based oscillators are also capable of operating from supply voltages at the order of 20 mV, as shown in Table 2. Recent publications suggest that topology can be used in the main power path due to the reasonable power efficiency even for operation around 100 mV.

To summarize, LC-based oscillators using native or depletion transistors have presented the lowest minimum voltages. However, the consumed area and the dependence of the inductor quality factor are the main constraints of this class of oscillators. On the other hand, CMOS-based oscillators occupying smaller areas are convenient for energy scavenging IC implementations, with room for $V_{DD}$ reduction. For the oscillator topologies presented in this review, a study related to the power conversion efficiency is necessary to increase the applicability of the circuits.

Table 1 Sub-100 mV fully-integrated oscillators.

| Ref. | Topology | $V_{DD,min}$ | Application |
|---|---|---|---|
| [13] | ES-XCO | 31 mV | Oscillator only |
| [13] | XCO | 46 mV | Oscillator only |
| [20] | IRO | 53 mV | Oscillator only |
| [37] | ST-RO | 53.2 mV | Oscillator only |
| [7] | ST-RO | 57 mV | Oscillator only |
| [6] | SI-RO | 57 mV | Start-up conv. |
| [40] | RO | 60 mV | Start-up conv. |
| [44] | Relaxation | 62 mV | Oscillator only |
| [48] | XCO | 65 mV | Start-up conv. |
| [42] | ST RO | 70 mV | Start-up conv. |
| [5] | RO | 80 mV | Start-up conv. |
| [12] | Colpitts | 86 mV | Oscillator only |
| [39] | RO | 95 mV | Start-up conv. |
| [22] | XCO | 100 mV | Start-up conv. |
| [4] | RO | 100 mV | Logic gates |

XCO – Cross-coupled oscillator;
ES-XCO – Enhanced-swing cross-coupled oscillator;
IRO – Inductive ring oscillator;
RO – Ring oscillator;
ST-RO – Schmitt trigger ring oscillator;
SI-RO – Stacked-inverter ring oscillator;

Table 2 Sub-100 mV oscillators using external components.

| Ref. | Topology | External components | $V_{DD,min}$ | Application |
|---|---|---|---|---|
| [3] | ES-XCO | 4 Induc. | 3.5 mV | Oscillator only |
| [26] | ES-XCO | 4 Induc. | 10 mV | Main conv. |
| [18] | ES-XCO | 4 Induc. | 11 mV | Start-up conv. |
| [47] | Cristal-based | Off-the-shelf + Transf. | 17 mV | Oscillator only |
| [11] | Colpitts | Off-the-shelf | 20 mV | Oscillator only |
| [30] | Trafo-based | Microtransf. | 20 mV | Start-up conv. |
| [49] | Hartley | Off-the-shelf | 20 mV | Main conv. |
| [34] | Trafo-based | MCM Off-chip microtransf. | 20 mV | Main conv. |
| [35] | Trafo-based | Transf. | 21 mV | Start-up conv. |
| [32] | Trafo-based | Off-chip microtransf. | 25 mV | Main conv. |
| [15] | Colpitts | 2 Induc. | 40 mV | Start-up conv. |
| [31] | Trafo-based | Transf. | 40 mV | Start-up conv. |
| [3] | XCO | 2 Induc. | 50 mV | Oscillator only |
| [45] | Pierce | 1 Crystal | 60 mV | Oscillator only |

## VII. Conclusion

This paper presented a systematic review of oscillators operating at DC voltages smaller than 100 mV. The analyses of LC and CMOS oscillators presented herein explored the theoretical limits of the minimum supply voltage of this class of circuits. Implementations of sub-100 mV circuits were reported covering the LC and CMOS oscillators, including the cross-coupled, enhanced-swing cross-coupled, Colpitts, transformer-based, and CMOS-based ring oscillators. Finally, a comparison between implementations reported in the literature, emphasizing minimum supply voltage, is presented. The analysis of the papers identified a lack of investigations related to power conversion efficiency and the applications to communication circuits.

## Acknowledgements

This work was supported in part by the Brazilian government agency, CNPq, National Council for Scientific and Technological Development.

## References

[1] M. B. Machado, R. L. Radin, M. C. Scheneider and C. Galup-Montoro, "A 20 µw, 50 mV, Fully-Integrated Cross-Coupled Oscillator for On-Body IoT Applications," in *NEWCAS*, 2021.

[2] M. Siniscalchi, N. Gammarano, C. Galup-Montoro, S. Bourdel and F. Silveira, "Minimum Supply Voltage of 2.45 GHz LCOscillator in 28 nm FD-SOI Process," in *NEWCAS*, 2021.

[3] M. B. Machado, M. C. Schneider and C. Galup-Montoro, "On the minimum supply voltage for MOSFET oscillators," *IEEE Transactions on Circuits and Systems I: Regular Papers*, vol. 61, no. 2, pp. 347-357, 2014.

[4] J. B. Burr and J. Shott, " A 200 mV self-testing encoder/decoder using Stanford ultra-low-power CMOS," in *Proceedings of IEEE International Solid-State Circuits Conference - ISSCC, pp. 84-85*, San Francisco, 1994.

[5] P.-H. Chen, X. Zhang, K. Ishida, Y. Okuma, Y. Ryu, M. Takamiya and T. Sakurai, "An 80 mV startup dual-mode boost converter by charge-pumped pulse generator and threshold voltage tuned oscillator with hot carrier injection," *IEEE Journal of Solid-State Circuits*, vol. 47, no. no. 11, pp. 2554-2562, 2012.

[6] T. A. S. Bose and M. L. Johnston, "Integrated cold start of a boost converter at 57 mV using cross-coupled complementary charge pumps and ultra-low-voltage ring oscillator," *IEEE Journal of Solid-State Circuits*, vol. 54, no. 10, pp. 2867-2878, 2019.

[7] L. A. P. Melek, M. C. Schneider and C. Galup-Montoro, "Operation of the classical CMOS schmitt trigger as an ultra-low-voltage amplifier," *IEEE Transactions on Circuits and Systems II: Express Briefs*, vol. 65, no. 9, pp. 1239-1243, 2018.

[8] M. Siniscalchi, F. Silveira and C. Galup-Montoro, "Ultra-low-voltage CMOS crystal oscillators," *IEEE Transactions on Circuits and Systems I: Regular Papers*, vol. 67, no. 6, pp. 1846-1856, 2020.

[9] D. Kleijer, "Oscillator with super low supply voltage," [Online]. Available: http://www.dicks-website.eu/fetosc/enindex.htm. [Accessed 04 2012].

[10] C. Galup-Montoro, M. C. Schneider and M. B. Machado, "Ultra-low-voltage operation of CMOS analog circuits:

amplifiers, oscillators and amplifiers," *IEEE Trans. Circuits Syst. II, Exp. Briefs,* vol. 59, pp. 932-936, 2012.

[11] F. R. d. Sousa, M. B. Machado and C. Galup-Montoro, "A 20 mV Colpitts Oscillator powered by a thermoelectric generator," in *IEEE International Symposium on Circuits and Systems (ISCAS),* Seoul, Korea (South), 2012.

[12] M. B. Machado, M. C. Schneider, D. L. Novack and C. Galup-Montoro, "Analysis and design of a fully-integrated Colpitts oscillator operating at ultra-low-voltages," *Analog Integr Circ Sig Process,* vol. 85, p. 27–36, 2015.

[13] M. B. Machado, M. Schneider and C. Galup-Montoro, "Fully integrated inductive ring oscillators operating at VDD below 2kT/q," *Analog Integr Circ Sig Process,* vol. 82, p. 5–15, 2015.

[14] M. B. Machado, F. Nornberg, M. Sawan, C. Galup-Montoro and M. C. Schneider, "Analysis and design of the Dickson charge pump for sub-50 mV energy harvesting," *Elsevier Microelectronics Journal,* vol. 90, pp. 253-259, 2019.

[15] B. Lim, J. Seo and S. Lee, "A Colpitts oscillator-based self-starting boost converter for thermoelectric energy harvesting with 40-mV startup voltage and 75% maximum efficiency," *IEEE Journal of Solid State Circuits ,* vol. 53, p. 3293–3302, 2018.

[16] D. Rozgić and D. Marković, "A Miniaturized 0.78-mW/cm2 autonomous thermoelectric energy-harvesting platform for biomedical sensors," *IEEE Transactions on Biomedical Circuits and Systems,* vol. 11, no. 4, pp. 773-783, 2017.

[17] H. Fuketa, S. -i. O'uchi and T. Matsukawa, "Fully integrated, 100-mV mini-mum Input voltage converter with gate-boosted charge pump kick-started by LC oscillator for energy harvesting," *IEEE Transactions on Circuits and Systems II: Express Briefs,* vol. 64, no. 4, pp. 392-396, 2017.

[18] R. L. Radin, M. Sawan, C. Galup-Montoro and M. C. Schneider, "A 7.5 mV-input boost converter for thermal energy harvesting with 11 mV self-startup," *IEEE Transactions on Circuits and Systems II: Express Briefs,* vol. 67, no. 8, pp. 1379-1383, Aug. 2020.

[19] A. K. Sinha, R. L. Radin, D. D. Caviglia, C. G. Montoro and M. C. Schneider, "An energy harvesting chip designed to extract maximum power from a TEG," in *2016 IEEE 7th Latin American Symposium on Circuits & Systems (LASCAS),* Florianopolis, 2016.

[20] M. B. Machado, M. C. Schneider and C. Galup-Montoro, "Analysis and design of ultra-low-voltage inductive ring oscillators for energy-harvesting applications," in *IEEE 4th Latin American Symposium on Circuits and Systems (LASCAS),* Cusco, Peru, 2013.

[21] S. M. Noghabaei and M. Sawan, "A fully integrated high-efficiency step-up DC-DC converter for energy harvesting applications," in *ISOOC,* 2016.

[22] H. Fuketa, S. -i. O'uchi and T. Matsukawa, "Fully integrated, 100-mV mini-mum Input voltage converter with gate-boosted charge pump kick-started by LC oscillator for energy harvesting," *IEEE Transactions on Circuits and Systems II: Express Briefs,* vol. 64, no. 4, pp. 392-396, 2017.

[23] D. Rozgić and D. Marković, "A Miniaturized 0.78-mW/cm2 autonomous thermoelectric energy-harvesting platform for biomedical sensors," *IEEE Transactions on Biomedical Circuits and Systems,* vol. 11, no. 4, pp. 773-783, 2017.

[24] M. C. Schneider and C. Galup-Montoro, CMOS Analog Design Using All-Region MOSFET Modeling, Cambridge: Cambridge University Press, 2010.

[25] H. O. Tabrizi, H. M. P. Jayaweera and A. Muhtaroglu, "Fully Integrated Autonomous Interface With Maximum Power Point Tracking for EnergyHarvesting TEGs With High Power Capacity," *IEEE Transactions on Power Electronics,* vol. 35, no. 5, pp. 4905-4014, 2020.

[26] M. B. Machado, M. Sawan, M. C. Schneider and C. Galup-Montoro, "10 mV – 1V step-up converter for energy harvesting applications," in *27th Symposium on Integrated Circuits and Systems Design (SBCCI),* 2014.

[27] M. B. Machado, M. Sawan, M. C. Schneider and C. Galup-Montoro, "Fully-integrated 86 mV–1V step-up converter for energy harvesting applications," in *IEEE 12th International New Circuits and Systems Conference (NEWCAS),* 2014.

[28] B.-M. Lim, J.-I. Seo and S.-G. Lee, "A Colpitts Oscillator-Based Self-Starting Boost Converter for Thermoelectric Energy HarvestingWith 40-mV Startup Voltage and75% Maximum Efficiency," *IEEE Journal of Solid-State Circuits,* vol. 53, no. 11, pp. 3293-3302, 2018.

[29] M. Lallart, L. V. Phung and B. Massot, "Transformer-Free, Off-the-Shelf ElectricalInterface for Low-Voltage DC Energy Harvesting," *IEEE Transactions on Industrial Electronics,* vol. 65, no. 7, pp. 5580-5589, 2018.

[30] Linear Technology, "LTC3108 Datasheet," [Online]. Available: https://www.analog.com/media/en/technical-documentation/data-sheets/LTC3108.pdf.

[31] J. P. Im, S. W. Wang, S. T. Ryu and G. H. Cho, "A 40 mV transformer-reuse self-startup boost converter with MPPT control for thermoelectric energy harvesting," *IEEE Journal of Solid-State Circuits,* vol. 47, no. 12, p. 3055–3067, Dec. 2012.

[32] P. Garcha, D. El-Damak, N. Desai, J. Troncoso, E. Mazotti, J. Mullenix, S. Tang, D. Trombley, D. Buss, J. Lang and A. Chandrakasan, "A 25 mV-StartupCold Start System WithOn-Chip Magnetics for Thermal Energy Harvesting," in *47th European Solid State Device Research Conference,* Louvain, 2017.

[33] A. Salah-Eddin, M. Vlad, D. Nicolas, V. Christian, A. Bruno and C. François, "Self-Powered Ultra-low Power DC-DC Converter for RF Energy Harvesting," in *IEEE Faible Tension Consommation*, 2012.

[34] A. Telles, M. B. Machado, M. M. Rocha and R. Teixeira, "Ultralow Voltage Power Converter Using a Microtransformer in MCM Technology," in *11$^{th}$ Workshop on Circuits and Systems Design (WCAS)*, 2021.

[35] Y. K. Teh and P. K. T. Mok, "Design of transformer-based boost converter for high internal resistance energy harvesting sources with 21 mV self-startup voltage and 74% power efficiency," *IEEE Journal of Solid-State Circuits,* vol. 49, no. 11, p. 2694–27, Nov. 2014.

[36] Y. Qian, J. H. D. Lu and Z. Hong, "An On-Chip Trans-former-Based Self-Startup Hybrid SIDITO Converter for Thermoelectric Energy Harvesting," *IEEE Transactions on Circuits and Systems II, Express Briefs,* vol. 65, no. 11, p. 1673–1677, 2018.

[37] J. Ferreira and C. Galup-Montoro, "Ultra-low-voltage CMOS ring oscillators," *Electronics Letters,* vol. 55, no. 9, p. 523–525, 2019.

[38] J. Meindl and J. Davis, "The fundamental limit on binary switch-ing energy for terascale integration," *IEEE J. Solid-State Circuits,* vol. 35, no. 11, p. 1515–1516, 2000.

[39] P. Chen, K. Ishida, K. Ikeuchi, X. Zhang, K. Honda, Y. Okuma, Y. Ryu, M. Takamiya and T. Sakurai, "Startup techniques for 95 mV step-up converter by capacitor pass-on scheme and VTH-Tuned oscillator with fixed charge programming," *IEEE Journal of Solid-State Circuits,* vol. 47, no. 5, p. 1252–1260, 2012.

[40] M. Dezyani, H. Ghafoorifard, S. Sheikhaei and W. A. Serdijn, "A 60 mV Input Voltage, Process Tolerant Start-Up System

for Thermoelectric Energy Harvesting," *IEEE Transactions on Circuits and Systems I: Regular Papers,* vol. 65, no. 10, p. 3568–3577.

[41] M. Ashraf and N. Masoumi, "A Thermal Energy Harvesting Power Supply with an Internal Startup Circuit for Pacemakers," *IEEE Transactions on Very Large Scale Integration (VLSI) Systems,* vol. 24, no. 1, pp. 26-37, 2017.

[42] J. Goeppert and Y. Manoli, "Fully Integrated Startup at 70 mV of Boost Converters for Thermoelectric Energy Harvesting," *IEEE Journal of Solid State Circuits,* vol. 51, no. 7, p. 1716–1726, 2016.

[43] S. B. a. M. L. Johnston, "A Stacked-Inverter Ring Oscillator for 50 mVFully-Integrated Cold-Start of Energy Harvesters," in *ISCAS*, 2018.

[44] T. D. Fernandes, C. Galup-Montoro and M. C. Schneider, "Analysis and design of the three-inverter schmitt trigger for supply voltages down to 50 mV," *IEEE Transactions on Circuits and Systems II: Express Briefs,* vol. 68, no. 7, p. 2302–2306, 2021.

[45] M. Siniscalchi, F. Silveira and C. Galup-Montoro, "Ultra-low-voltage CMOS crystal oscillators," *IEEE Transactions on Circuits and Systems I: Regular Papers,* vol. 67, no. 6, pp. 1846-1856, 2020.

[46] Y. Zeng, T. Jang, Q. Dong, M. Saligane, D. Sylvester and D. Blaauw, "A 1.7nW PLL-Assisted Current Injected 32KHz Crystal Oscillator for IoT," in *EEE Solid-State Circuits Society*, Kyoto, 2017.

[47] A. M. Korolev, V. M. Shulga and O. G. Turutanov, "Ultra-low supply voltage crystal quartz oscillator," *Review of Scientific Instruments,* vol. 67, 2021.

[48] D. Rozgic and D. Markovic, " A Miniaturized 0.78-mW/cm2 autonomous thermoelectric energy-harvesting platform for biomedical sensors," *IEEE Transactions on Biomedical Circuits and Systems,* vol. 11, no. 4, pp. 773-783, 2017.

[49] M. Lallart, L. V. Phung and B. Massot, "Transformer-Free, Off-the-Shelf Electrical Interface for Low-Voltage DC Energy Harvesting," *IEEE Transactions on Industrial Electronics*, vol. 65, no. 7, p. 5580–5589, 2018.